AAPT PHYSICS EDUCATION | AMERICAN JOURNAL of PHYSICS

The Fermi atomic pseudopotential

Marvin L. Cohen

Citation: American Journal of Physics **52**, 695 (1984); doi: 10.1119/1.13572
View online: http://dx.doi.org/10.1119/1.13572
View Table of Contents: http://scitation.aip.org/content/aapt/journal/ajp/52/8?ver=pdfcov
Published by the American Association of Physics Teachers

[2]See his 1954 letter to the Wilhelm Busch Society in Germany, W. Busch Jahrb. **33**, 56 (1967).
[3]See H. Dukas and B. Hoffmann, *Albert Einstein: The Human Side* (Princeton University, Princeton, NJ, 1979), pp. 78 and 130.
[4]See, for example, "Wo ich geh und wo ich steh," Ref. 3, p. 124.
[5]W. Busch, *Klecksel the Painter*, translated by M. Born (Ungar, New York, 1965).
[6]W. Busch, *Werke*, edited by F. Bohne (Standard-Verlag, Hamburg, 1959), Vol. IV, p. 208. This and all subsequent passages from Busch's works were translated by the authors who would be happy to supply interested parties with the original versions of all German texts quoted.
[7]W. Busch, *Sämtliche Briefe*, edited by F. Bohne (W.-Busch-Gesellschaft, Hannover, 1968–69), Vol. II, p. 64.
[8]Ref. 6, Vol. III, pp. 259–260.
[9]Reference 6, p. 52.
[10]*The Genius of Wilhelm Busch*, edited and translated by Walter Arndt (University of California Press, Berkeley and Los Angeles, 1982), p. 153.
[11]Reference 6, pp. 28–29.
[12]Reference 6, p. 186.
[13]For a detailed analysis, see B. and D. Lotze, W. Busch Jahrb. **42**, 28–35 (1976).
[14]Reference 6, p. 167.
[15]Reference 6, p. 169.
[16]Reference 6, pp. 183–184.
[17]Reference 6, p. 184.
[18]Reference 6, p. 184.
[19]Reference 6, pp. 184–185.
[20]Reference 6, p. 189.
[21]Reference 6, p. 266.
[22]Reference 6, p. 165.
[23]Reference 6, p. 317.
[24]"Der Nöckergreis," Ref. 6, p. 204.
[25]Reference 6, Vol. I, pp. 500–503.
[26]Reference 6, pp. 274–277.

The Fermi atomic pseudopotential

Marvin L. Cohen
Department of Physics, University of California, and Materials and Molecular Research Divison, Lawrence Berkeley Laboratory, Berkeley, California 94720

(Received 1 September 1983; accepted for publication 18 November 1983)

A discussion of Fermi's calculation using the pseudopotential approach is given. This is followed by a brief review of some of the principal extensions and applications of atomic pseudopotentials to condensed matter physics in the following 50 years.

I. INTRODUCTION

Fifty years ago Fermi[1,2] introduced the atomic pseudopotential and scattering length concepts to explain the observations of Amaldi and Segrè[3] on the shifts of alkalai atomic spectral lines when the vapor samples were mixed with foreign gases. The theory explained both the sign and magnitude of the measured shifts in addition to providing the important theoretical tools mentioned above. Although the pseudopotential has had a significant impact on atomic and condensed matter physics, there has been less awareness of Fermi's contribution to the atomic potential than his application[4] of the pseudopotential approach to nuclei.

The discussion in this paper will focus on the atomic pseudopotential and explore extensions and applications of this concept. We begin by discussing the essential features of Fermi's original work, and then describe a few of the principal developments of pseudopotential theory. Finally, the focus will be on current accomplishments resulting from the use of pseudopotentials in condensed matter physics.

II. FERMI'S CALCULATION

The experiments of Amaldi and Segrè[3] indicated that the higher terms of the alkalai atomic spectra were more sensitive to the presence of a foreign gas than the lower terms. The size of the shift and its sign depended on the nature of the foreign gas. Fermi[1] attributed the observations to two physical effects, polarization and scattering. The first effect arises because an electron in a large orbit can experience the dielectric screening of the foreign gas. Fermi calculated this shift Δ_ϵ which expressed in wavenumbers is given by

$$\Delta_\epsilon = +20[(\epsilon-1)/18\pi^2\hbar c]e^2n^{1/3}, \quad (1)$$

where ϵ is the dielectric constant of the foreign gas and n is the number of foreign gas atoms per unit volume. The $+$ sign signifies a red shift, and the magnitude is approximately one wavenumber for foreign gases at pressures of the order of one atmosphere.

If the foreign gases do not have permanent electric dipole moments, as was the case in the experiments of Amaldi and Segrè, then the effect was of the same magnitude as calculated using Eq. (1). However, some gases could give a blue shift, and it is the scattering effect which explains this aspect. The scattering effect is calculated to be of the same order as Δ_ϵ, and it can have either sign. It was the calculation of this effect which motivated Fermi to introduce the pseudopotential, and it is this part of Fermi's calculation on which we will focus.

The outer electron of the host alkalai atom experiences a slowly varying potential U from the rest of the atom and stronger potentials V_i arising from the foreign gas atoms. The V_i are deep and narrow (radius ρ) compared with the

wavelength of the outer electron. Hence the wave function ψ for the outer electron will be slowly varying except for localized irregularities near the perturbing atoms. Fermi therefore introduces another function $\bar{\psi}$ which is an average wave function in a region small compared to the electron's wavelength but large enough to contain a substantial number of foreign gas atoms. This function $\bar{\psi}$ reproduces the general trend of ψ without the irregularities.

The Schrödinger equation for ψ is

$$\left(\frac{-\hbar^2}{2m}\nabla^2 + U + \sum_i V_i\right)\psi = E\psi. \tag{2}$$

By averaging as described above, the Schrödinger equation for $\bar{\psi}$ is

$$\frac{\hbar^2}{2m}\nabla^2\bar{\psi} + (E - U)\bar{\psi} - \sum_i V_i\psi = 0. \tag{3}$$

Working with the radial part of the wave function $u(r) = r\psi(r)$ Fermi obtains an estimate of the last term in Eq. (3). This is done by employing the approximation shown in Fig. 1, i.e.,

$$u(r) = (a + r)\bar{\psi}. \tag{4}$$

Since the second term in Eq. (3) is much smaller than the third, within the radius ρ of one foreign atom potential well, to lowest order,

$$(-\hbar^2/2m)u''(r) + V(r)u(r) = 0. \tag{5}$$

Integrating Eq. (5) and using Eq. (4) we find

$$(2m/\hbar^2)\bar{V}\bar{\psi} = -4\pi a\bar{\psi}. \tag{6}$$

Hence the last term in Eq. (3) for n potential wells per unit volume is

$$\sum_i V_i\psi = (-2\hbar^2\pi an/m)\psi \tag{7}$$

and this shifts the energy E by

$$\Delta_a = 2\hbar^2\pi an/m. \tag{8}$$

This term gives a red shift for $a > 0$ and a blue shift for $a < 0$.

Converting to wavenumbers and adding the contributions from Eq. (1) and (8) we have

$$\Delta = [20(\epsilon - 1)e^2/16\pi^2\hbar c]n^{1/3} + \hbar an/mc. \tag{9}$$

The total shift Δ given by Eq. (9) corresponds to Eq. (22) of Fermi's paper. Hence in this classic work Fermi has explained the observed shift in the spectral lines via two effects, he has introduced the scattering length a, and he has invented the pseudopotential. We will focus on the latter approximation which comes in through the use of $\bar{\psi}$, Fig. 1, and the averaging processes given by Eqs. (4)–(6).

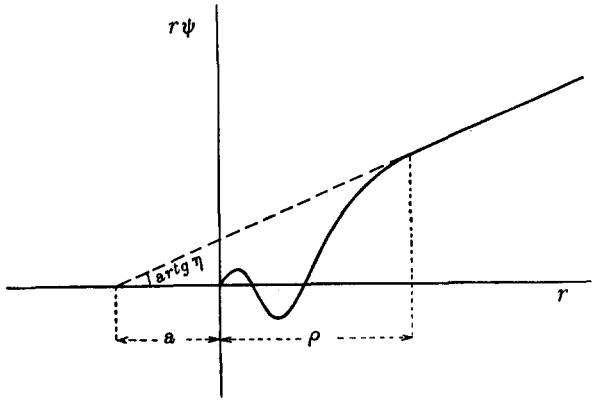

Fig. 1. Fermi's pseudopotential approximation.

III. THE NEXT 30 YEARS

Another early pseudopotential reference is the work of Hellmann[5] who used this approximation to reproduce atomic and molecular energy levels. Schemes similar to Hellmann's were later developed further and used even in the 1960's.[6] However the next main thrust in pseudopotential research came from studies of solids. One important question which pseudopotential theory helped to answer was: Why does the nearly free electron theory work so well for solids? In other words, why is it possible to use weak potentials and smooth plane wave like wave functions to represent the interactions of conduction electrons in metals?

It was the work of Phillips and Kleinman[7] using the orthogonalized plane-wave method (OPW) of Herring[8] which demonstrated why the nearly free electron model works. The OPW scheme was developed to provide a method to calculate the electronic band structure of a solid, i.e., the energies of the electrons in the solid as a function of their wave vector, $E(k)$. The dilemma of band structure calculations is that near a positive core (nucleus plus core electrons) the valence electrons experience a strong potential and are atomic-like. Between the cores, the potential is fairly constant, and hence the valence electron wave functions should be fairly smooth in this region. Therefore an atomic-like basis set is appropriate near the cores while plane waves are more suitable between the cores.

Herring proposed that a plane wave which was made orthogonal to the core states would have several desirable properties. Near the core it would resemble the next higher state above the core states since it is orthogonal to all the states in the core. Between the cores where the potential is small and slowly varying, the plane-wave nature of the state would be appropriate. These OPW's formed a good basis set for electronic structure calculations particularly for metals. Just a few OPW's in an expansion set for a wave function representing valence electrons in a solid were sufficient to compute many electronic properties accurately.

Phillips and Kleinman used the OPW approach to formulate a pseudopotential in the following way. Let ψ be the true wave function representing the valence electrons, and partition ψ into a smooth part ϕ which is the pseudowave function and a component made out of core states ϕ_c; hence,

$$\psi = \phi + \sum_c b_c\phi_c. \tag{10}$$

For a specific application, the smooth part of the wave function ϕ can be expanded in plane waves, and the crystal symmetry can be taken into account.

Following the OPW approach the state ψ is made orthogonal to the core states

$$\langle\phi_c|\psi\rangle = 0, \tag{11}$$

hence

$$b_c = -\langle\phi_c|\phi\rangle, \tag{12}$$

and

$$\psi = \phi - \sum_c \langle\phi_c|\phi\rangle\phi_c. \tag{13}$$

If we now operate on ψ with the total Hamiltonian H, then the eigenvalues E obtained should be the true eigenvalues for the valence electrons moving in the crystal potential, i.e.,

$$H\psi = E\psi. \tag{14}$$

Using Eq. (13),

$$H\phi - \sum_c \langle \phi_c | \phi \rangle E_c \phi_c = E\phi - E\sum_c \langle \phi_c | \phi \rangle \phi_c, \tag{15}$$

where the E_c are the eigenvalues for the core electron states. Rearranging terms, we have

$$H\phi + \sum_c (E - E_c)\phi_c \langle \phi_c | \phi \rangle = E\phi. \tag{16}$$

Equation (16) can be written in the following form:

$$(H + V_R)\phi = E\phi, \tag{17}$$

where

$$V_R\phi = \sum_c (E - E_c)\phi_c \langle \phi_c | \phi \rangle \tag{18}$$

is a repulsive potential which keeps the valence electrons out of the core. This potential originates from the orthogonality terms in the OPW-like wave function. Hence it arises from the Pauli principle and represents the "Pauli force" which pushes the valence electrons away from the core.

When the repulsive potential is added to the attractive Coulomb potential from the positive core, the sum is a net weak potential or pseudopotential, i.e., starting with Eq. (17) we now have

$$(p^2/2m + V_c + V_R)\phi = E\phi \tag{19}$$

or

$$(p^2/2m + V)\phi = E\phi, \tag{20}$$

where V_c is the attractive core potential and V is the net weak pseudopotential. An important property of Eq. (20) is that even though it represents a Schrödinger equation with a pseudopotential and a pseudowave function, the eigenvalue obtained is the real energy E which was the eigenvalue solution of Eq. (14).

Hence a scheme is obtained in which a weak potential and a smooth wave function which can be expanded in plane waves yields the real eigenvalues for the valence electrons in a crystalline solid. Therefore the use of the nearly free electron model is justified. Some caution in using V should be exercised since V_R is non-Hermitian, ϕ is not normalized, and V is nonunique, but studies[9,10] in the 1960's gave prescriptions and guidance on how to deal with these problems.

Although considerable research was done to study the Phillips–Kleinman and other variations of the pseudopotential discussed above, direct applications of this approach to real systems were scarce. A complete calculation of V_R as it is given here involves many of the same calculations as the OPW approach. Therefore the main impact of the Phillips–Kleinman result was conceptional. For applications, model or empirical pseudopotentials were introduced, and these were very successful in dealing with applications to real materials.

IV. EMPIRICAL AND MODEL POTENTIALS

The introduction and use of empirical[11] and model[13] potentials as pseudopotentials has had a profound effect on solid-state physics during the past 20 years. Electronic structure calculations for metals, semiconductors, semimetals, and insulators were done successfully. The empirical approach led to an unraveling of reflectivity spectra, photoemission properties, chemical bonding, energy band structures, etc. (see Refs. 10–15).

Basically two approaches were followed in fitting the potentials. One was to model the real space (Fig. 2) potential as a function of position; the other involved using approximations to the Fourier transformed potential as a function of wave vector or momentum (Fig. 3). The simplest real space models are straightforward once the Phillips–Kleinman calculation is known. Since the attractive and repulsive potentials essentially cancel in the core region then the real space potential should be a constant near the core and Coulombic outside. Hence a simple model potential would be (see Fig. 2)

$$V(r) = -Ze/r, \quad r > r_c, \tag{21}$$

$$= -Ze/r_c, \quad r \leqslant r_c, \tag{22}$$

where Z is the valence and r_c is the core radius. A more popular choice is the empty core pseudopotential

$$V(r) = -Ze/r, \quad r > r_c, \tag{23}$$

$$= 0, \quad r \leqslant r_c. \tag{24}$$

These simple potentials give surprisingly good results for electronic structure especially when one considers that only a one parameter fit is used.

Heine and coworkers[12] extended and refined the above model potentials by allowing the constant potential in the core to vary instead of fixing it at zero or $-Ze/r_c$. The constant was taken to be a function of the angular momentum and energy of the electronic state under investigation. These potentials became known as "model potentials," and the parameters were fit to atomic spectra. When used for calculations in a solid the model potentials were screened by the valence electrons by using a dielectric function. Tables of potentials[13] became available, and model potentials were used for many elements, particularly metallic systems.

The second approach was to fit[11,13–17] the Fourier coefficients or form factors of the potentials. For a periodic solid the Fourier transform of the pseudopotential becomes a Fourier sum over reciprocal lattice vectors[18] $\mathbf{G}$,

$$V(\mathbf{r}) = \sum_{\mathbf{G}} S(\mathbf{G}) V_a(\mathbf{G}) e^{i\mathbf{G}\cdot\mathbf{r}} \tag{25}$$

where the $V_a(\mathbf{G})$ represents the Fourier transform of the atomic pseudopotential at wave vector $\mathbf{q} = \mathbf{G}$. These form factors can be obtained from a Fourier analysis of the model potential or fit to experiment. When the experimental input is used, the method is called the Empirical Pseudopotential Method (EPM). The structure factor[18] $S(\mathbf{G})$ locates the atoms in a unit cell; it is obtained from an x-ray analysis of the solid,

$$S(\mathbf{G}) = \sum_{\tau} e^{-i\mathbf{G}\cdot\tau}, \tag{26}$$

where τ is a basis vector to each of the atoms in the unit cell.

Hence the structure is regarded as input, and only the form factors $V_a(\mathbf{G})$ are needed to obtain the potential and in turn the energy eigenvalues and wave functions. If the ex-

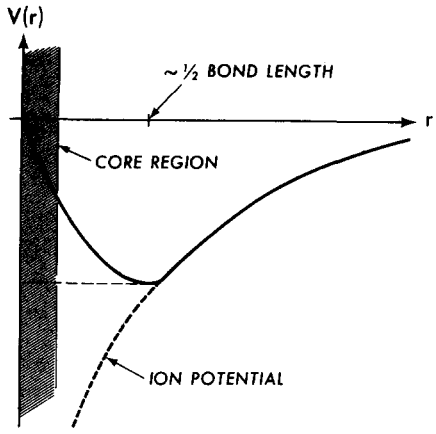

Fig. 2. Schematic pseudopotential in real space.

pansion of Eq. (25) did not converge, it would take too many parameters to fit $V(\mathbf{r})$, and this scheme would not be tenable. However, because of the cancellation of the core potential in the core region the form factors of Eq. (25) become small for large $\mathbf{G}$ (which corresponds to small distances). In fact, for most elements, three parameters or form factors are sufficient to fit the potential (Fig. 3).

A good example is Si which exists in the diamond structure where each of the cores are tetrahedrally coordinated and the valence electrons form the covalent bonds. If the Si pseudopotential is expanded in the reciprocal lattice following Eq. (25), then only three form factors corresponding to $G^2 = 3$, $G^2 = 8$, and $G^2 = 11$ are needed to fix the potential. With these three numbers, the electronic band structure can be obtained to 1% to 2% accuracy over a range of 1 Ry. Similarly for other semiconductors with diamond and zincblende structure like Ge, GaAs, ZnSe, etc. three parameters per element are sufficient to give an adequate description of their electronic properties.

The fitting of the parameters relied heavily on optical data. Unlike the atomic spectra used by Fermi, reflectivity spectra of solids are normally broad. For this reason interpretation of these spectra in terms of electron transitions was more difficult, and there was a considerable time lag between the interpretation of solid-state spectra compared

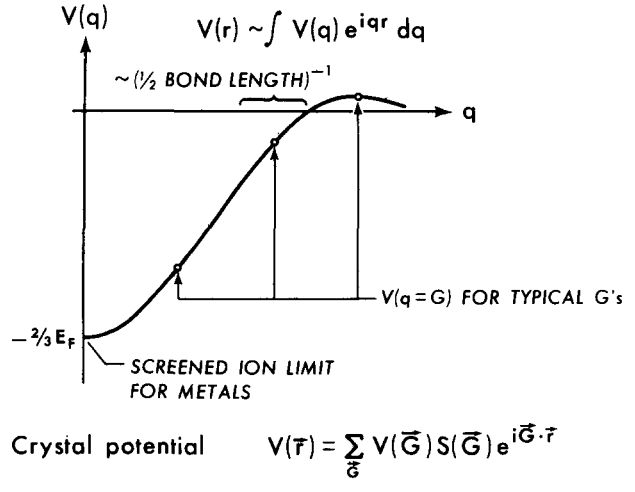

Fig. 3. Schematic pseudopotential in reciprocal space where G is a reciprocal lattice vector, $S(G)$ is the structure factor, and $V(G)$ is the pseudopotential form factor.

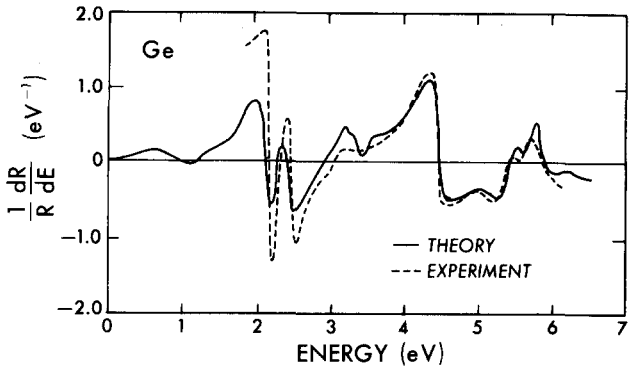

Fig. 4. Calculated modulated reflectivity for Ge compared to experiment. The experimental results are due to R. R. L. Zucca and Y. R. Shen, Phys. Rev. B **1**, 2668 (1970).

to atomic spectra. Modulation or derivative spectroscopy[19] provided sharper spectra, and this was very helpful. A typical example for Ge is given in Fig. 4.

The EPM procedure (Fig. 5) was to compare a calculated spectrum with its measured counterpart and to fit the pseudopotential form factors to produce agreement. Photoemission data were also used prominently; however angular resolved photoemission spectra (ARPES) were not available when most of the studies were done. ARPES can be used to measure $E(\mathbf{k})$ which is a severe test of the theory. Fortunately the EPM predictions agree with later ARPES data, and this stands as an excellent test of the method (Fig. 6).

Another area where the EPM provided important physical insight is in chemical bonding.[10] By using the wave functions obtained in an EPM calculation, it was possible to compute the electronic charge density[20] as a function of position in space for each band n or for the sum of all the valence bands, i.e.,

$$\rho_n(\mathbf{r}) = \sum_{\mathbf{k}} |\phi_{n,\mathbf{k}}(\mathbf{r})|^2, \tag{27}$$

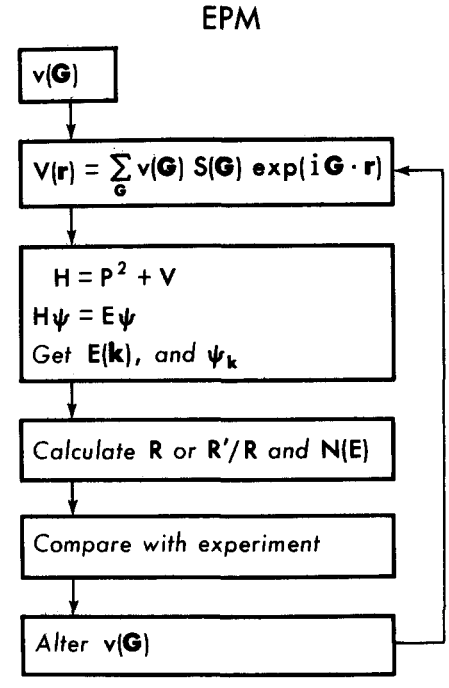

Fig. 5. The empirical pseudopotential method.

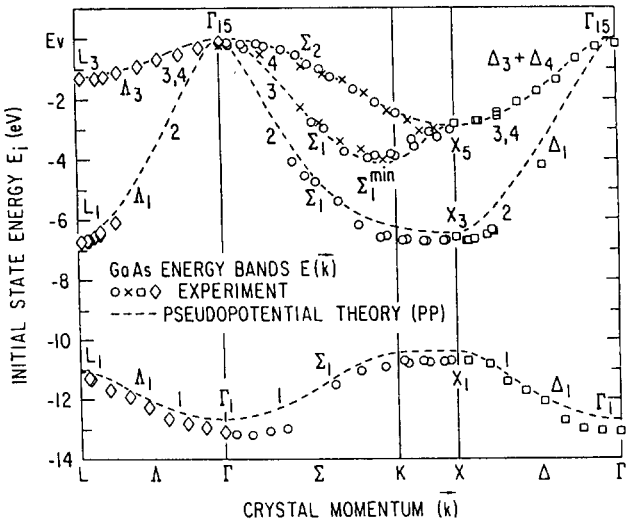

Fig. 6. Comparison of the pseudopotential band structure for GaAs [J. C. Phillips and K. C. Pandey, Phys. Rev. Lett. **30**, 787 (1973)] with measured angular resolved photoemission spectra [T. C. Chiang, J. A. Knapp, M. Aono, and D. E. Eastman, Phys. Rev. B **21**, 3513 (1980)].

where $\phi_{n,k}(\mathbf{r})$ is the wave function for the state $\mathbf{k}$ in a band n which is occupied. The total charge density is given by

$$\rho_{\text{tot}}(\mathbf{r}) = \sum_{N} \rho_n(\mathbf{r}), \tag{28}$$

where the sum is over all the occupied valence bands. Once again the EPM calculations served as predictions of the charge distributions. Experimental analysis came later, and the agreement between experiment and theory is excellent (Fig. 7).

Dozens of crystals were analyzed using the EPM. Band

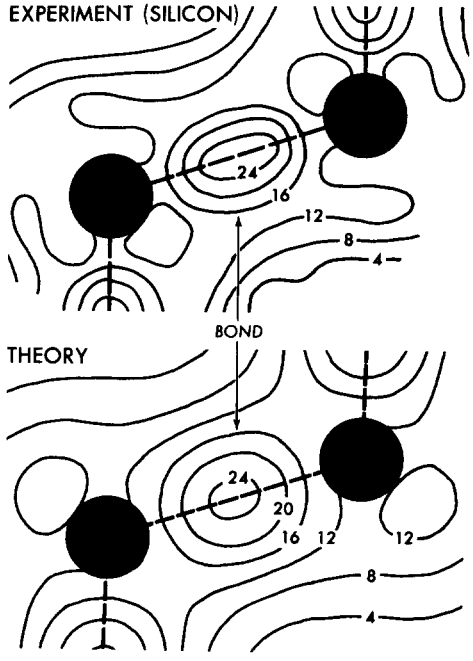

Fig. 7. Total calculated valence charge density for Si representing the sum of the individual band contributions. The comparison with x-ray measurements was made by L. W. Yang and P. Coppens, Solid State Comm. **15**, 1555 (1974).

structures, optical and photoemission spectra, charge distributions, bond charges, dielectric functions, Debye–Waller factors, etc. were calculated, and large amounts of experimental data were analyzed and interpreted.

V. SELF-CONSISTENT PSEUDOPOTENTIALS

In the 1970's experiments in surface science became more reliable and reproducible, and this motivated theorists to attempt calculations for surfaces and interfaces. The EPM was not directly extendable to surfaces for two reasons. First, the EPM relied on periodicity, and a surface breaks translational invariance. The arrangement of the atoms at the surface, the adjacent vacuum, and the rearrangement of the valence electrons make the surface different from the bulk. This latter aspect brings in the second major problem. Since the pseudopotential is fit in the EPM, it contains the electron–core and the electron–electron interaction. Therefore when only part of the potential changes at a surface and it is not clear how to change the potential in the EPM to lower order, it is the electron–electron interaction which has the major change at a surface or interface because of the redistribution of valence electrons at the interface, and the electron–core interaction can be assumed unchanged from the bulk.

One way to solve the periodicity problem is through the use of supercells. A large cell is constructed using the structure factor given in Eq. (26). A slab of material is modeled with vacuum above and below, and this supercell is repeated. Each supercell has two surfaces, and the properties of these surfaces mimic a solid surface. We can now use all the tools of Fourier sums and deal with an infinite number of surfaces.

The electronic charge redistribution and its effects on the potential can be evaluated by separating the total potential into a core part and a valence electron part. The core part or ionic potential is used as input, but the electronic part of the potential is calculated using the charge density $\rho(r)$. This potential has two parts: a screening or Hartree contribution and an exchange-correlation contribution. The Hartree potential can be obtained from the electron charge density using Poisson's equation. In principle, the exchange-correlation potential is more complex; however, there are approximations to this potential which use only the electron density as input[21] (see Fig. 8).

Using the supercell, electron-core pseudopotential, and the electron–electron potential calculated using the methods described above, it is possible to compute properties of localized configurations like surfaces and interfaces.[21] If the proper unit cell is chosen the model structure in the supercell can be used to simulate an atom, molecule, defect, impurity, etc. The calculation is done in the following manner (see Fig. 8). First an EPM potential is used as input to generate the charge density which in turn gives the Hartree and exchange-correlation potential. The structure and electron-core pseudopotential is added, and the new potential is used as input. After about six cycles the input and output potentials or charge densities are the same, and the calculation is said to be "self-consistent."

For the surface calculation, on the first cycle the charge tends to flow out of the surface. However this redistribution of charge produces a potential which pulls charge back in on the next cycle. After a few more cycles the changes are negligible. The charge and potentials become stationary,

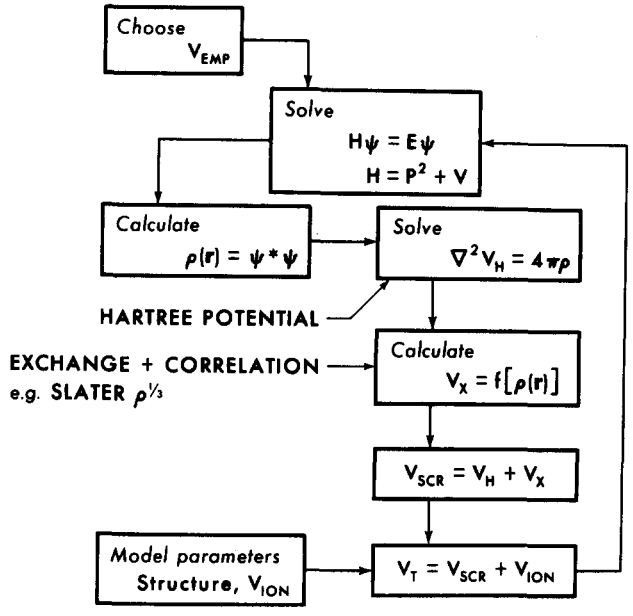

Fig. 8. Block diagram for calculating self-consistent potentials for surfaces and interfaces.

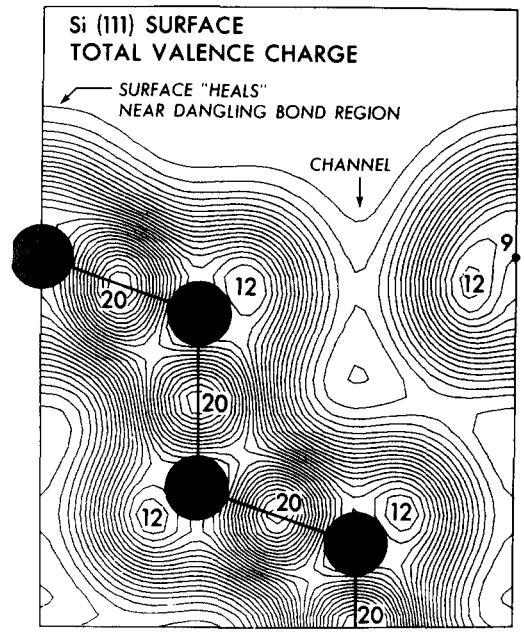

Fig. 10. Total valence charge density for an ideal unrelaxed Si(111) surface. Charge contours are plotted in the (110) plane and normalized to e per primitive cell. Shaded circles represent atomic cores.

and the results of this model calculation represent real surfaces.

One of the first applications of this self-consistent pseudopotential approach was to Si(111).[22] If Si is oriented along the [111] direction and the bonds are cut, then a (111) surface is exposed. This surface has been studied more than any other with modern experimental and theoretical techniques. In Fig. 9 a ball and stick model illustrating the geometry of the Si(111) surface is given. In Fig. 10 a self-consistent charge density plot illustrates the electron distribution at and near the surface. A few layers into the surface the bonds strongly resemble the bulk bonds calculated using the EPM (Fig. 7). At the surface "cut bond" is not seen. The charge in the surface "half-bond" redistributes and produces a smooth charge density at the surface. In effect the cut is healed. Channels through the surface into the bulk of the crystal exist (Fig. 10), and these represent the paths for impurity atoms which enter and form interstitial impurities in Si.

There are also surface states; i.e., electron states which exist only near the surface. These surface states decay into the bulk solid and into the vacuum above. They are localized by the almost discontinuous surface potential, and they dominate the electronic properties of the surface. The charge density of Fig. 10 does not illustrate these states since bulk states dominate here. However it is straightforward to use the results of the self-consistent pseudopotential calculation to illustrate[22] the properties of the surface states.

A number of surfaces, interfaces, and other localized configurations were studied in the 1970's using the method described above.[21] The calculations required the structure (i.e., position of the cores) of the configuration of interest as input. The structural part was not calculated using pseudopotentials. Often the structure was difficult to obtain. For example for Si(111), the case considered, the ideal or (1×1) structure is known not to be correct when the surface is treated in the standard manner. Two prominent structures are the (2×1) and the (7×7) varieties, and these must be used as input before the above calculation can be done.

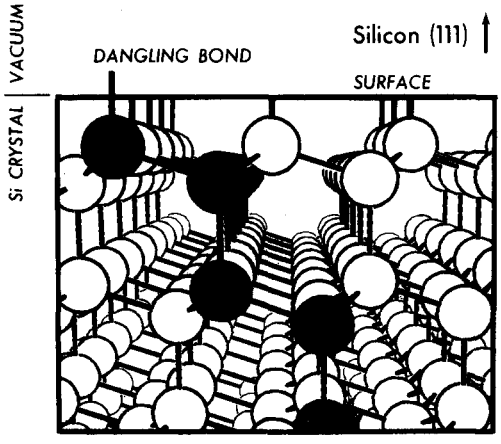

Fig. 9. Ball and stick model for the Si(111) surface.

VI. FIFTY YEARS LATER

The limitations of the EPM and self-consistent approaches discussed above have been removed in the 1980's.[23] Current pseudopotential schemes require only the atomic number as input, and no information about the solid is used to generate the potential. In addition, it is possible to calculate crystal structure both for bulk and surface geometries. Because of these refinements, a number of new applications are now possible.

Ab initio pseudopotentials are obtained from atomic wave functions. Standard computer programs are generally available to produce atomic wave functions for core and valence electron states using the atomic number as input. To generate a pseudopotential the pseudowave function for

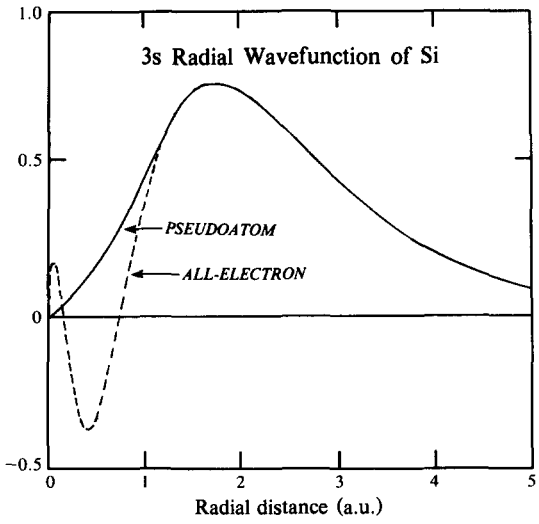

Fig. 11. Comparison of the 3*s* pseudowave function and all-electron wave function for Si.

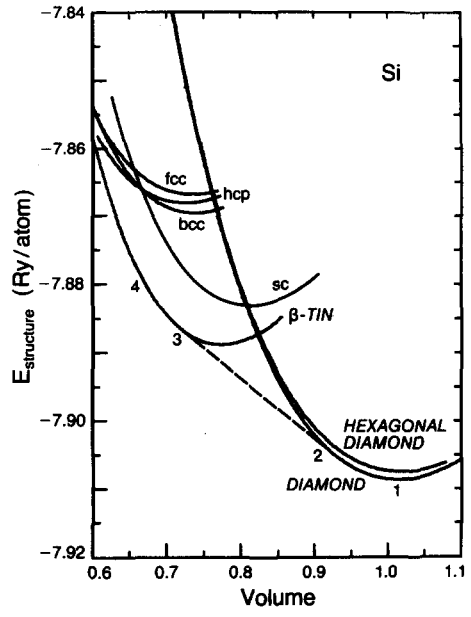

Fig. 12. Total energy curves for seven structures of Si as a function of volume normalized to the experimental volume. The dashed line is the common tangent between the diamond and white tin phases.

the valence electron state of interest is constrained to reproduce precisely the all electron wave function at large distances away from the core, but the wave function is taken smoothly to zero near the core region. As shown in Fig. 11 for the Si 3*s* wave function, the pseudowave function differs from the all-electron wave function at distances less than that corresponding to the outermost maximum. The pseudowave function is nodeless—it lacks oscillations in the core region. It is interesting to compare Fig. 11 with Fig. 1. Several schemes for constructing pseudopotentials to produce these wave functions are available.[24–29]

Hence the electron–core pseudopotential can be determined using the atomic wave function. The Hartree and exchange-correlation potentials can be obtained using the density as discussed previously. There are several functionals which can be used to generate the exchange–correlation potentials and the density functional approach[30] has been very successful especially for determining ground state properties of solids.

The total energy for a solid in a given configuration can now be evaluated using the techniques described. Electron–core, electron–electron, and exchange-correlation energies are obtained from the pseudopotential and charge density. The core–core and electron kinetic energies can be evaluated using Madelung sums and the electron wave function. It is convenient and conceptually straightforward to compute these quantities in momentum space,[31] and hence the only input are the atomic number and the crystal structure of interest.

Returning to Si as a prototype solid the total energy was computed[32] for a variety of crystal structures. In the subset of diamond, hexagonal diamond, simple cubic (sc), white tin, body centered cubic (bcc), hexagonal close pack (hcp), and face centered cubic (fcc), the diamond structure has the lowest energy (Fig. 12). By varying the volume, v, and calculating the energy for each structure, the $E(v)$ curves give the lattice constant for the minimum energy in each structure. For the diamond structure the value of the lattice constant is in remarkable agreement with experiment (Table I). The curvature near the minimum energy yields information about the compressibility or bulk modulus of the solid. If the lattice constant is made large enough to simulate a collection of isolated atoms, the total energy difference between this configuration and the solid with its normal lattice constant gives the cohesive energy of the solid.

Table I lists the results for Si, Ge, and C. The lattice constants, bulk moduli, and cohesive energies are in excellent agreement with experiment. Similar calculations have been done for other semiconductors, metals, and insulators with comparable results.

Solid–solid structural phase transitions can also be examined using the $E(v)$ curves calculated from the *ab initio* pseudopotentials. For example, for Si at smaller volumes the white tin (β-tin) structure has lower energy than the diamond structure, and a structural transition should therefore occur as a function of pressure. In contrast hexagonal diamond is above cubic diamond over the entire range of volume, hence a structural transition will not occur, and the hexagonal modification can be made only in a metastable phase.

Referring to Fig. 12 the dashed line represents the common tangent between diamond and β-tin. At point 1 Si is in

Table I. Static structural properties for Si, Ge, and C.

	Lattice constant (Å)	Cohesive energy (eV)	Bulk modulus (Mbar)
Si			
Calc.	5.45	4.67	0.98
Expt.	5.43	4.63	0.99
% Diff.	0.4%	1%	−1%
Ge			
Calc.	5.66	4.02	0.73
Expt.	5.65	3.85	0.77
% Diff.	0.1%	4%	−5%
C			
Calc.	3.60	7.57	4.41
Expt.	3.57	7.37	4.43
% Diff.	0.8%	3%	−1%

the diamond structure, but if compressed to 0.928 of its volume, at point 2 it begins the transition to β-tin. At point 3 which corresponds to a fractional volume of 0.718 the transition is complete, and at point 4 the system is in the β-tin structure. The calculated transition volumes are within around 1% of experiment,[32] and the slope of the common tangent gives a good calculational estimate of the transition pressure.

Lattice vibrational frequencies or phonons can also be obtained[33] using the pseudopotential total energy scheme. Empirical models for phonons often assume force constants or springs of various strengths connecting the atoms. Calculations of this kind require interactions up to 15 neighbors to achieve suitable accuracy for Si. The total energy approach uses only the atomic number and mass as input. One method for obtaining the vibration spectrum is to assume a phonon or a specific vibrational state is "frozen in" and the crystal is distorted. The total energy of this distorted state is then compared with the ideal arrangement where the atoms are in their equilibrium positions. This energy difference is related to the phonon energy (Table II). Another method involves the calculation of the forces on planes of atoms when one plane is moved. These energy or force methods lead to calculations of the phonon spectrum which are in excellent agreement with experiment. Even the pressure dependencies of the various phonon modes (Gruneisen constants) are given accurately by this *ab initio* approach (Table II).

The above calculations of the properties of a solid–solid phase transition and the phonon spectra have been extended to other semiconductors, to insulators, and to metals. Hence the pseudopotential total energy technique is generally applicable to solids, and the results are highly accurate for calculating lattice constants, bulk moduli, cohesive energies, phonons, and parameters related to structural phase transitions. Most static structural properties can be calculated with this method. However, because a local density functional approach is used for determining the exchange-correlation potentials, excited state properties like semiconductor band gaps are not given accurately in this scheme. Modifications are needed or EPM-like calculations can be done.

Currently there is considerable activity in attempting to use the pseudopotential total energy approach to predict crystal structures. The hope is that it may be possible to predict the existence of materials with desirable properties and then fabricate these systems. An example would be the prediction of a crystal structure for an element or compound which may be metastable. Then the use of pressure or temperature may be used to bring this substance to standard temperatures and pressures. Diamond is such a substance. The graphitic form of carbon has a lower energy than the diamond form, yet diamonds are found in nature.

Since there are many choices of structures to check for a given number of constituent elements, calculations of this kind are difficult. Some progress[34] is being made in predicting the surface structure or surface reconstructions by calculating total energies and forces at a surface. Since the calculations deal with two-dimensional models, the number of likely choices to consider is reduced. These surface calculations have motivated a considerable number of experimental investigations. Hopefully they will also evolve into schemes for predicting three-dimensional structures.

Hence it is fair to say that the Fermi atomic pseudopotential has come a long way in the past 50 years: from the early work on atoms in gases to the development of schemes to predict structural and electronic properties of atoms, solids, and molecules. There appear to be many more possible applications in the future. Not only will refinements of the techniques discussed here certainly be made, but if we extrapolate modestly, new important applications to fundamental and applied problems in condensed matter physics are very likely.

Table II. Total energy calculations of phonon energies and Grüneisen parameters for a few phonon frequencies of Si.

Si	LTO(Γ)	TA(X)	TO(X)	LOA(X)
Phonon freqs. (TH_z)				
$F_{calc.}$	15.16	4.45	13.48	12.16
$F_{expt.}$	15.53	4.49	13.90	12.32
Deviation	− 2.4%	− 0.9%	− 3.0%	− 1.3%
Grüneisen parameter				
$\gamma_{calc.}$	0.92	− 1.50	1.34	0.92
$\gamma_{expt.}$	0.98	− 1.40	1.50	~0.90

ACKNOWLEDGMENTS

I would like to thank E. Segrè for introducing me to Fermi's paper, for his translation of the paper, and for helpful discussions. I am also grateful to F. Bassani and D. Vanderbilt for helpful discussions. This work was supported by National Science Foundation Grant No. DMR7822465 and by the Director, Office of Energy Research, Office of Basic Energy Sciences, Materials Sciences Division of the U.S. Department of Energy under Contract No. DE-AC03-76SF00098.

Editor's Note: The translation of Fermi's 1934 paper by E. Segrè is available through the Physics Auxiliary Publication Service (PAPS) at AIP.

[1] E. Fermi, Nuovo Cimento **II**, 157 (1934).
[2] E. Segrè, *Collected Papers of E. Fermi* (University of Chicago, Chicago, 1962), p. 706.
[3] E. Almaldi and E. Segrè, Nuovo Cimento **II**, 145 (1934).
[4] E. Amaldi, O. D'Agostino, E. Fermi, B. Pontecorvo, F. Rasetti, and E. Segrè, Proc. R. Soc. (London), A **149**, 552 (1935).
[5] H. Hellmann, J. Chem. Phys. **3**, 61 (1935).
[6] R. G. Parsons and V. F. Weisskopf, Z. Fur Physik **202**, 492 (1967).
[7] J. C. Phillips and L. Kleinman, Phys. Rev. **116**, 287 (1959).
[8] C. Herring, Phys. Rev. **57**, 1169 (1940).
[9] B. J. Austin, V. Heine, and L. J. Sham, Phys. Rev. **127**, 276 (1962).
[10] W. Harrison, *Pseudopotentials in the Theory of Metals* (Benjamin, Reading, MA, 1966).
[11] M. L. Cohen and T. K. Bergstresser, Phys. Rev. **141**, 789 (1966).
[12] I. V. Abarenkov and V. Heine, Phil. Mag. **12**, 529 (1965).
[13] M. L. Cohen and V. Heine, Solid State Phys. **24**, 37 (1970).
[14] J. C. Phillips, *Bonds and Bands in Semiconductors* (Academic, New York, 1973).
[15] J. R. Chelikowsky and M. L. Cohen, Phys. Rev. **14**, 556 (1976).
[16] J. C. Phillips, Phys. Rev. **112**, 685 (1958).
[17] F. Bassani and V. Celli, J. Phys. Chem. Solids **20**, 64 (1961).
[18] C. Kittel, *Introduction to Solid State Physics* (Wiley, New York, 1976), 5th ed.
[19] M. Cardona, *Modulation Spectroscopy* (Academic, New York, 1969).
[20] M. L. Cohen, Science **179**, 1189 (1979).
[21] M. L. Cohen, Advances in Electronics and Electron Physics **51**, 1 (1980).

[22]M. Schlüter, J. R. Chelikowsky, S. G. Louie, and M. L. Cohen, Phys. Rev. B **12**, 4200 (1975).
[23]M. L. Cohen, Physica Scripta **T1**, 5 (1982).
[24]T. Starkloff and J. D. Joannopoulos, Phys. Rev. B **16**, 5212 (1977).
[25]A. Zunger and M. L. Cohen, Phys. Rev. B **18**, 5449 (1978).
[26]D. R. Hamann, M. Schlüter, and C. Chiang, Phys. Rev. Lett. **43**, 1494 (1979).
[27]G. Kerker, J. Phys. C **13**, L189 (1980).
[28]S. G. Louie, S. Froyen, and M. L. Cohen, Phys. Rev. B **26**, 1738 (1982).
[29]M. T. Yin and M. L. Cohen, Phys. Rev. B **25**, 7403 (1982).
[30]P. Hohenberg and W. Kohn, Phys. Rev. **136**, B864 (1964); W. Kohn and L. J. Sham, Phys. Rev. **140**, A1333 (1965).
[31]J. Ihm, A. Zunger, and M. L. Cohen, J. Phys. C **12**, 4401 (1979).
[32]M. T. Yin and M. L. Cohen, Phys. Rev. B **26**, 5668 (1982).
[33]M. T. Yin and M. L. Cohen, Phys. Rev. B **26**, 3259 (1982).
[34]J. E. Northrup and M. L. Cohen, Phys. Rev. Lett. **49**, 1349 (1982).

PROBLEM

Sometimes the most familiar problems in physics contain interesting aspects that are seldom pointed out in standard treatments. Consider the Kepler problem—a particle attracted to a fixed center by an inverse-square-law force.

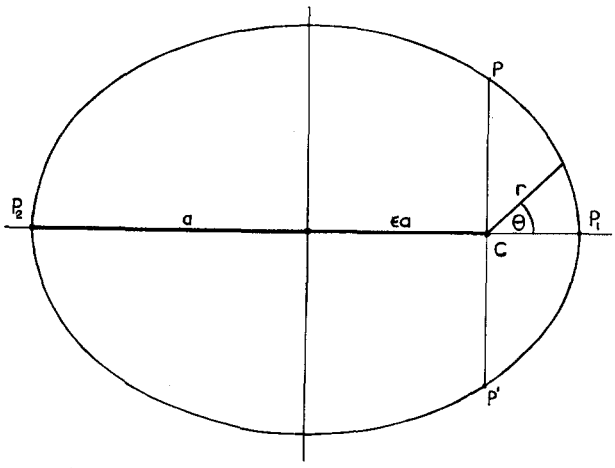

Fig. 1. Ellipse in polar coordinates with turning points P_1 and P_2 and points of maximum radial speed P and P'.

We all know that the bounded orbits of the particle are in general ellipses, with one focus at the attracting center, denoted by C in Fig. 1. Standard discussions emphasize the turning points of the motion P_1 and P_2, where r, the distance of the particle from the force center, takes on its extremal values. By energy conservation, we know that the particle speed is a maximum at P_1 and a minimum at P_2.

But what about the *radial speed* $|\dot{r}|$ of the particle relative to the force center? Clearly $|\dot{r}|$ is zero at the turning points and hence maximal somewhere in between. By symmetry, if the radial speed has a maximum at a point P on the orbit, it will reach that same maximum at a point P' obtained by reflection through the ellipse major axis. What is interesting—and constitutes the problem posed to the reader—is to show that the line connecting P and P' actually *passes through the force center*, as illustrated in Fig. 1. (Solution is on page 761.)